






Article

Use of *Silybum marianum* Extract and Bio-Ferment for Biodegradable Cosmetic Formulations to Enhance Antioxidant Potential and Effect of the Type of Vehicle on the Percutaneous Absorption and Skin Retention of Silybin and Taxifolin

Edyta Kucharska ^{1,*}, Richard Sarpong ¹, Anna Bobkowska ², Joanna Ryglewicz ², Anna Nowak ³,
Łukasz Kucharski ³, Anna Muzykiewicz-Szymańska ³, Wiktoria Duchnik ³ and Robert Pelech ¹

¹ Department of Chemical Organic Technology and Polymeric Materials, Faculty of Chemical Technology and Engineering, West Pomeranian University of Technology in Szczecin, Pulaski Ave. 10, 70-322 Szczecin, Poland; srpngrchrd@gmail.com (R.S.); robert.pelech@zut.edu.pl (R.P.)

² NISHA Karol Ryglewicz, Jana Kasprowicza Ave. 4, 62-040 Puszczykowo, Poland; anna.bobkowska@nisha.com.pl (A.B.); joanna.ryglewicz@nisha.com.pl (J.R.)

³ Department of Cosmetic and Pharmaceutical Chemistry, Pomeranian Medical University in Szczecin, 70-111 Szczecin, Poland; anna.nowak@pum.edu.pl (A.N.); lukasz.kucharski@pum.edu.pl (Ł.K.); anna.muzykiewicz@pum.edu.pl (A.M.-S.); wiktoria.duchnik@pum.edu.pl (W.D.)

* Correspondence: edyta.kucharska@zut.edu.pl; Tel.: +48-888-615-273

Abstract: In the present study, extract (E) and bio-ferment (B) were obtained from ground and defatted thistle seeds of *Silybum marianum*. Their antioxidant activity was assessed using the DPPH, ABTS, and FRAP techniques, while total polyphenols were measured by the Folin–Ciocalteu method. High antioxidant activity was found in both the E (0.91 mmol Trolox/L ± 0.2) and B (1.19 mmol Trolox/L ± 0.2) using DPPH methods, so the obtained cosmetic raw materials were incorporated into hydrogel and organogel substrates to obtain cosmetic formulations with antioxidant activity. However, there is a scarcity of research providing information on the skin penetration of the main active components of *S. marianum*, which have an antioxidant effect. Therefore, we assessed in vitro the penetration through pig skin of the main components contained in the obtained B and E, such as silybin and taxifolin, which are part of the silymarin complex. We also used pure silymarin (S) for comparison. Among the tested preparations, H-S showed the utmost significant penetration of taxifolin, having a cumulative permeation of $87.739 \pm 7.457 \mu\text{g}/\text{cm}^2$. Biodegradation tests of the prepared formulations were also performed, containing cosmetic raw materials and S. Studies of the effect of the cosmetic formulations on aerobic biodegradation showed a good level of degradation for the prepared formulations, some of which (O-B and O-S) were classified as easily degradable (OECD).

Keywords: bio-ferment; biodegradable natural cosmetics with *Silybum marianum*; antioxidant activity of bioactive compounds; skin penetration; biodegradability



Citation: Kucharska, E.; Sarpong, R.; Bobkowska, A.; Ryglewicz, J.; Nowak, A.; Kucharski, Ł.; Muzykiewicz-Szymańska, A.; Duchnik, W.; Pelech, R. Use of *Silybum marianum* Extract and Bio-Ferment for Biodegradable Cosmetic Formulations to Enhance Antioxidant Potential and Effect of the Type of Vehicle on the Percutaneous Absorption and Skin Retention of Silybin and Taxifolin. *Appl. Sci.* **2024**, *14*, 169. <https://doi.org/10.3390/app14010169>

Academic Editor: Burkhard Poeggeler

Received: 1 December 2023

Revised: 18 December 2023

Accepted: 22 December 2023

Published: 24 December 2023



Copyright: © 2023 by the authors. Licensee MDPI, Basel, Switzerland. This article is an open access article distributed under the terms and conditions of the Creative Commons Attribution (CC BY) license (<https://creativecommons.org/licenses/by/4.0/>).

1. Introduction

Selected plant raw materials rich in active components are commonly used in the production of natural cosmetics. The active ingredients contained in plant raw materials (i.e., polyphenolic compounds, proteins, amino acids, carbohydrates, or phospholipids) show antioxidant activity and influence the appropriate hydration of the skin. Extracts obtained from selected plant raw materials are characterized by favorable skin properties, offering the potential to be used as cosmetic raw materials. Bio-ferments, which contain innovative active ingredients derived from natural plant raw materials (but also plant extracts or organic oils) during microbial fermentation, are characterized by a range of

properties related to their antioxidant activity, moisturizing, or anti-allergenic effects. Bio-fermented oils, which are excellent emollients rich in active compounds, are characterized by their sebum-regulating effects. The main advantage of bio-ferments as innovative ingredients in cosmetic formulations, which are obtained by microbial fermentation, is their high biocompatibility. In addition, technological and environmental factors, such as the reduction in carbon footprint and the use of waste materials (including plant biomass), mean that bio-ferments are increasingly being used in the cosmetic industry. The microbial fermentation of plant raw materials makes it possible to obtain cosmetic raw materials with better properties regarding their biological activity, antioxidant activity, or suppression of tyrosinase than those of non-fermented raw materials (such as plant extracts). In addition, bio-ferments have great potential as innovative cosmetic raw materials with a high SPF. Plant raw materials may prove effective in the treatment of skin hyperpigmentation due to the inhibition of melanogenesis through the activation of 3-kinase [1–9].

Silymarin is composed of a complex of compounds, mainly flavonoids, with a high level of biological activity. Flavonolignans are formed in plants by the oxidative coupling of the flavonoid taxifolin with a coniferyl alcohol. The main compounds in the complex are silybin and isosilybin as well as silychristin and silydianin. Lesser amounts of other flavonolignans are included in the complex: isosilychristin, silymonine, slandrins, and silygermine. Silymarin and preparations containing it are often standardized for the silybin content. However, the low water solubility and the limited permeability of silymarin through the skin have significantly limited the use of this active ingredient as a cosmetic raw material in topicals. Therefore, researchers are seeking to increase the solubility of silymarin and thus increase its bioavailability. One possible solution is to incorporate this active substance into suitable cosmetic vehicles applied topically to the skin. Examples of cosmetic vehicles include gel substrates such as hydrogels and organogels—biodegradable and non-degradable vehicles of active substances devoid of their own pharmacological activity—into which the active substances can be placed. Thanks to the specific structure of the gels, they form a skeletal reservoir for the storage of therapeutic substances, released under the influence of certain external stimuli but protected from the harmful effects of the environment [10–16].

Milk thistle (*Silybum marianum*) is a native Mediterranean plant used for medicinal and ornamental purposes. Mainly the fruits of this plant are used for medicinal purposes. Silymarin, a compound from milk thistle, is non-toxic and has no adverse effects when administered orally. Silymarin, a polyphenolic compound, has been found to have therapeutic effects through regenerative, antioxidant, and anti-inflammatory mechanisms. Silymarin inhibits xanthine oxidase activity and NADPH oxidase activity, affecting the oxidoreductive status of cells and signal transduction pathways. It stimulates the activation of the cell antioxidant enzymes catalase and superoxide dismutase, reducing glutathione levels. It also prevents hepatocyte damage in rats under various environmental conditions. Silymarin has been found to have an anti-inflammatory effect not only in the liver but also in mice, preventing septic shock and reducing the secretion of nitric oxide, reactive oxygen species, interleukin-1 β , and prostaglandin E2. It has also been shown to protect neurons by inhibiting the release of nitric oxide, TNF- α , and superoxide anion radicals by microglia cells. This protective effect may be beneficial in preventing inflammatory neurodegenerative conditions like Parkinson's disease, Alzheimer's disease, and multiple sclerosis. Silymarin has also been found to inhibit UV-induced NF- κ B activation in keratinocytes, potentially preventing sunburn, inflammation, and skin damage induced by UV exposure, which may lead to cancer. Silybin can be used to create products that shield the skin from UV rays, such as cosmetic creams, and is of significant interest in the cosmetics industry, particularly for anti-aging and anti-free radical products. In the presence of phospholipids, silybin can undergo transformations, forming complexes better able to traverse the biomembrane [17–22].

Gels used as vehicles for active substances show a few advantages: their ease of preparation, limited amount of excipients, low overall cost of producing the finished

formulation, increased resistance to moisture, organic nature that prevents the development of microbial contaminants, increased skin penetration and facilitated particle transport, generally low toxicity, and non-irritant nature when introducing hydrophilic and lipophilic compounds into the vehicle [23–28].

Permeability is mostly determined by the skin barrier. The largest obstruction to the flow of molecules and the transfer of active substances is the *stratum corneum*, the outermost layer of the skin. Its chemical composition is mostly composed of ceramides, fatty acids, cholesterol and its derivatives, and minute quantities of phospholipids. The low solubility of silymarin in aqueous solutions, which leads to limited bioavailability and low absorption rates, is a major barrier to investigating new uses for it. A few studies have addressed the biodegradation of formulations containing silymarin, extract, and bio-ferment using activated sludge. The use of microorganism activity in our experiment is to assess the ability of formulations to degrade (in aerobic conditions) and determine whether they have a high degree of persistence in the environment. The OECD suggested a technique for testing the capacity for aerobic degradation, which is evaluated by measuring the CO₂ emitted. The formulations are categorized as easily or weakly biodegradable. This kind of vehicle is crucial for obtaining the bioavailability, high solubility, and permeability of active substances. Organogels and hydrogels are employed in this research study as vehicles. This study aims to find suitable vehicle(s) for silymarin, extract, and bio-ferment of milk thistle due to silymarin's poor skin permeability and low solubility. The originality of this study consists in its in-depth analysis of hydrogel and organogel formulations' biodegradation processes, as well as its evaluation of their environmental effects. The most appropriate vehicle(s) that are bioavailable and improve silymarin solubility and skin permeability can be chosen because of this investigation. Moreover, the use of the extract and bio-ferment from *Silybum marianum* in cosmetic preparations increased the antioxidant potential of the obtained formulations. Our evaluation of the pig skin permeation of the main components of bio-ferment and extract, which are part of the silymarin complex, showed the influence of the type of carrier on the transdermal absorption and retention of silibinin and taxifolin in the skin.

2. Materials and Methods

2.1. Materials

6-hydroxy-2,5,7,8-tetramethylchroman-2-carboxylic acid (Trolox), 2,4,6-tripyridyl-s-triazine (TPTZ), 2,2-diphenyl-1-picrylhydrazyl (DPPH), and a medium for lactic acid bacteria (CM039) were acquired from Sigma Aldrich (Sigma-Aldrich Merck Group, St. Louis, MO, USA). Gallic acid and Folin–Ciocalteu reagent were purchased from Merck, Darmstadt (Germany). Acetic acid (99.5%), glycerin, methanol (96%), and phosphate-buffered saline (PBS; pH 7.00 ± 0.05) were purchased from Chempur (Piekary Śląskie, Poland). Acetonitrile (J.T. Baker brand) for HPLC was purchased from Avantor Performance Materials Poland S.A. (Gliwice, Poland). Hydroxyethylcellulose was purchased from Mazidla.com (Poznań, Poland). Silymarin, silybin, taxifolin, isopropyl myristate, and Pluronic F-127 were acquired from Sigma-Aldrich (St. Louis, MO, USA). Soy lecithin was acquired from Nanga (Karagen Kappa, Warszawa, Poland). All reagents used were of analytical grade.

Chempur (Piekary Śląskie, Poland) provided the acetic acid, ethanol (96%), methanol, phosphate-buffered saline (PBS, pH 7.4), potassium hydroxide (KOH), dipotassium hydrogen phosphate (K₂HPO₄), sodium phosphate dibasic dihydrate (Na₂HPO₄·2H₂O), ammonium chloride (NH₄Cl), magnesium(II) sulfate heptahydrate (MgSO₄·7H₂O), calcium chloride dihydrate (CaCl₂·2H₂O), potassium hydroxide (KOH), sodium hydroxide (NaOH), barium hydroxide (Ba(OH)₂), orthophosphoric acid (H₃PO₄), and iron (III) chloride hexahydrate (FeCl₃·6H₂O). Formic acid was acquired from Supelco (Bellefonte, PA, USA) (98–100% for HPLC LiChropur™). Eucerin was provided by Fagron (Krakow, Poland), and zinc paste was provided by Aflofarm (Pabianice, Poland). Every reagent was of analytical quality.

A medium for lactic acid bacteria (CM0359) was purchased from OXID (M.R.S. BROTH, Rogosa, Sharpe). Strains of lactic acid bacteria (*Lactobacillus reuteri* MI_0168, *Lactobacillus salivarius* LY_0652, *Lactobacillus brevis* LY_1120, *Lactobacillus acidophilus* MI-0078, *Lactobacillus rhamnosus* MI-0272, *Lactobacillus plantarum* MI-0102, and *L. rhamnosus* LY-0457) were purchased from Probiotal (NOVARA). BIO cane molasses (NatVita) was purchased from Mirków, Poland. Lipase AY30 was purchased from Thermo Scientific (Białystok, Poland). Sodium dodecyl sulfate (SDS; Sigma-Aldrich, 99.0%) is a substance that is frequently used in biodegradation research as both a benchmark and a positive control [28].

2.2. Plant Materials

Ground and defatted grains of plant material (milk thistle) were purchased from Slodkie Zdrowie (Białystok, Poland).

2.3. The Milk Thistle Bio-Ferment and Extract Preparation

Preparation of the bio-ferment (B) of milk thistle (ground and defatted grains):

Stage 1. Preparation of the inoculum

A total of 750 mL of distilled water was introduced into a 1000 mL flask, the flask was heated until it boiled and kept at this temperature for 2 h (to sterilize the apparatus), and then the contents of the flask were cooled to 60 °C. After this time, 50.00 g of lactic acid bacteria medium (CM0359) was introduced into the flask and heated (to its boiling point) for 2 h, and then the contents of the flask were cooled to a temperature of 37.5 °C in order to introduce lactic acid bacteria strains (700.00 mg). The introduced bacterial strains were multiplied for 48 h at 37.5 °C, thus obtaining the inoculum. A mixture of lactic acid bacteria strains was used in the fermentation process because the ultimate outcome of mixed fermentation is superior to that of fermentation carried out with a single isolated strain (there is a synergistic effect from different bacterial strains). Compared to a single strain, the use of mixed bacterial cultures increases the efficiency of the process with better use of plant raw materials. Additionally, there is an increased ability to adapt the strains used to changing process conditions, with increased resistance to contamination by undesirable microorganisms. The use of mixed bacterial culture is a technique that not only enhances fermentation efficiency but also yields economic advantages. Due to the absence of the requirement to isolate a specific strain, the overall expenses of the entire procedure are reduced, and the fermentation time is shortened [29,30].

Stage 2. The milk thistle fermentation process and filtration of the obtained bio-ferment

The following raw materials were introduced into a 500 mL conical flask: molasses (18.00 g); distilled water (300.00 g); mineral salts such as ammonium sulfate (2.00 g), calcium chloride (1.00 g), and potassium dihydrogen phosphate (1.00 g); Lipase AY30 enzyme (70.00 mg); ground and defatted milk thistle grains (5.00 g); and inoculum (10.00 mL). The contents of the flask were stirred for 30 min (until the introduced raw materials were dissolved), and then the fermentation process was started in a laboratory dryer at a temperature of 37.5 °C for an appropriate time. During the process, samples were taken every day and analyzed for polyphenol content (see Section 2.7.4: Total polyphenol content). The highest content of polyphenols was observed on the 21st day of fermentation, after which a gradual decrease in antioxidant activity (content of active compounds) was observed. Therefore, the process was carried out for 21 days, performing three independent experiments [29,31].

After the process was completed, the obtained bio-ferment was subjected to 3-stage filtration: I: first, the bio-ferment was filtered in a glass funnel; II: then the bio-ferment was centrifuged in a centrifuge (5 min, 166 Hz, 10,000× g); III: finally, the additionally filtered and centrifuged bio-ferment was filtered using sterile syringe filters with a pore size of 0.45 µm (intended for sterilizing filtration of aqueous solutions). In this way, the cosmetic raw material was free of microorganisms. The amount of bio-ferment obtained and filtered was approximately 100 mL. The bio-ferment was stored in a freezer at −15 °C for 3 months.

Preparation of the extract (E) of milk thistle (ground and defatted grains):

Extraction of ground and defatted grains of milk thistle was carried out using an ultrasonic method. First, 300.00 mL of distilled water was introduced into 5.00 g of the ground and defatted grains of milk thistle. Next, the extraction was carried out with the use of ultrasound bath at a frequency of 40 kHz (for 1 h at 60 °C), and then the extract obtained was subjected to filtration on a pressure funnel through a Whatman paper filter (codified EEA03).

2.4. Hydrogel (H-B, H-E) and Organogel (O-B, O-E) Preparation

The hydrogels (H) containing bio-ferment (B) or extract (E) of milk thistle were prepared based on a revised methodology developed by Makuch et al. [32]. Hydroxyethyl cellulose (HEC) and glycerin were added to the bio-ferment for milk thistle (or extract), water was replaced, and they were mixed with a magnetic stirrer (WIGO MS 11 HS with a heating function, Stargard, Poland) at a stirring speed of 4.17 Hz. The polymer solution was heated to a temperature of 60 °C, and the mixture was cooled to ambient temperature under continuous agitation.

The organogels (O) containing bio-ferment (B) and extract (E) of milk thistle were prepared as follows: the oil phase, which consists of soya lecithin, was created by dissolving its components in a suitable amount of isopropyl myristate (using a temperature of 50 °C and a WIGO MS 11 HS magnetic stirrer with a heating function, Stargard, Poland).

To prepare the aqueous phase, the specified quantities of Pluronic F-127 were dissolved in the bio-ferment of milk thistle (or extract), and water was replaced at a temperature of 50 °C. The aqueous phase was slowly added drop-wise to the oil phase with continuous stirring for a few minutes. In this way, organogels were obtained. The formulations were obtained using high-speed mechanical homogenization (IKA®T18 digital Ultra Turrax, IKA, Bionovo, Legnica, Poland) at 367 Hz.

In this stage, two hydrogels containing bio-ferment or extract, namely H-B and H-E; a control containing pure silymarin (S) at a concentration of 1% (H-S); two organogels containing bio-ferment or extract, namely O-B and O-E; and a control containing pure silymarin O-S are used. The hydrogel and organogel formulations are detailed in Table 1.

Table 1. Constituents of the hydrogels and organogels utilized in this investigation.

Ingredient	H-B	H-E	H-S
Silymarin	-	-	8.13
Bio-ferment/Extract	86.32	86.32	-
HEC	3.16	3.16	2.44
Glycerin	10.53	10.53	8.13
Water	-	-	81.30
Ingredient	O-B	O-E	O-S
Silymarin	-	-	1.69
Bio-ferment/Extract	68.67	68.67	-
Soy lecithin	3.43	3.43	3.38
Pluronic F-127	10.73	10.73	10.55
Isopropyl myristate	17.17	17.17	16.88
Water	-	-	67.51

HEC—hydroxyethylcellulose; Amount of the components is expressed in g.

2.5. The Stability of Hydrogels and Organogels

The stability of all formulations (H-B, H-E, H-S, O-B, O-E, and O-S) was tested as in the previous studies [33]. Specifically, the separation of all formulations was evaluated by a centrifuge test. The vehicle samples (10.00 g) were centrifuged (MPW-223e, Mechanika Precyzyjna, Warsaw, Poland) at 1750 × g, subjecting the preparation to a temperature of 25 °C for a duration of 10 min in order to see if it could be broken down. Moreover, the stability of all vehicles was also evaluated using the heating–cooling test: incubation at 45 °C (DHG-9075A drying oven) for 48 h, followed by incubation at 4 °C (in the refrigerator)

for 48 h. The experiment was conducted over a span of six cycles. The stability of all formulations kept at centrifugation and heating–cooling conditions were confirmed by their visual appearance.

2.6. Wettability of Hydrogel and Organogel

To study the effect of the bio-ferment (B), extract (E), and pure silymarin (S) on all formulations' wettability, the Kruss 165 DSA100 drop shape analyzer (Filderstadt, Germany) was used. One drop of distilled water (4 μ L) was placed on the preparation's surface, and the contact angle of the sessile drop method was measured using DSA4 software-controlled. The examination of the contact angle was conducted 5 s after placing the drop on the formulation. Measurements were made on the surface of the formulation with a layer thickness of 100 μ m. The formulations from ten different places were measured, and the outcomes were calculated by taking the average (c.a._{av.}) as shown in Figure 1a–h.

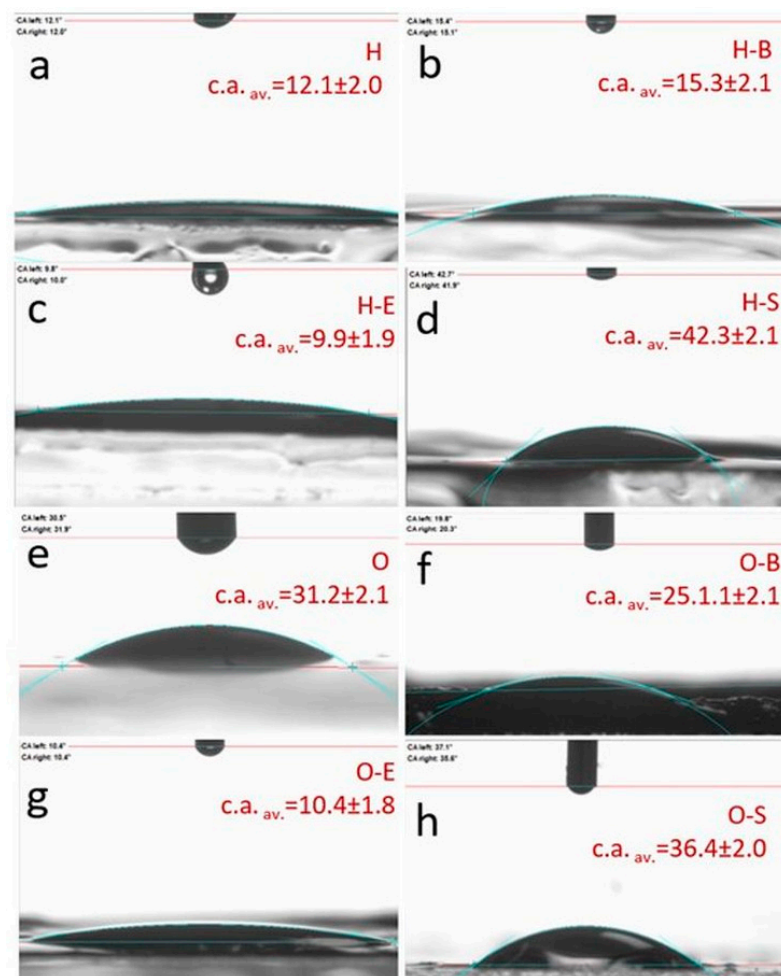


Figure 1. Contact angle (c.a._{av.}) of the formulations: (a) H $12.1^{\circ} \pm 2.0$; (b) H-B $15.3^{\circ} \pm 2.1$; (c) H-E $9.9^{\circ} \pm 1.9$; (d) H-S $42.3^{\circ} \pm 2.1$; (e) O $31.2^{\circ} \pm 2.1$; (f) O-B $25.1^{\circ} \pm 2.1$; (g) O-E $10.4^{\circ} \pm 1.8$; (h) O-S $36.4^{\circ} \pm 2.0$.

2.7. Antioxidant Activity and Total Polyphenols Content of Silymarin, Bio-Ferment, and Extract

2.7.1. DPPH Radical Scavenging Assay

To assess the antioxidant potential of silymarin, bio-ferment, and extract, the DPPH method was used [34]. The analyses were conducted on the Thermo Scientific GENESYS 50 apparatus at the wavelength $\lambda = 517$ nm. Trolox (6-hydroxy-2,5,7,8-tetramethylchroman-2-carboxylic acid) served as a benchmark material. The antioxidant activity was expressed

in mmol Trolox/L of appropriate cosmetic raw material, based on the resulting calibration curve $y = -1.2463x + 1.0546$ ($R^2 = 0.999$).

First, a 1% ethanolic solution of silymarin was prepared. The antioxidant activity of the prepared solution and the obtained bio-ferment (B) and extract (E) was measured as follows: 2.85 mL 0.3 mmol/L alcoholic solution containing about 1.000 ± 0.020 (at $\lambda = 517$ nm) of the DPPH radical was inserted into the tube, and 0.15 mL of the ethanolic solution of silymarin or cosmetic raw materials obtained (B or E) was added. Control samples devoid of antioxidants were generated using the same methodology. The tubes were wrapped in aluminum foil, sealed with a stopper, and then incubated for 10 min at room temperature. Three independent experiments were performed, and each sample was analyzed three times.

2.7.2. ABST Method

To determine the antioxidant capacity of silymarin, bio-ferment, and extract, the ABTS method was used [34]. The analyses were conducted with the Thermo Scientific GENESYS 50 (Fisher Scientific, Warszawska, Poland) apparatus at the wavelength $\lambda = 734$ nm. Trolox (6-hydroxy-2,5,7,8-tetramethylchroman-2-carboxylic acid) was used as a reference substance. The antioxidant activity was quantified and reported as mmol Trolox/L of appropriate cosmetic raw material based on the resulting calibration curve $y = -1.2718x + 0.9924$ ($R^2 = 0.999$).

First, 1% ethanolic solution of silymarin was prepared. The antioxidant activity of the prepared solution and the obtained bio-ferment (B) and extract (E) was measured as follows: 2.50 mL solution of the ABTS with an absorbance of about 1.000 ± 0.020 at $\lambda = 734$ nm was placed in the tube, and 0.025 mL of the ethanolic solution of silymarin or obtained cosmetic raw materials was added. Control samples devoid of antioxidant were generated using the same methodology. The tubes were encased in aluminum foil and were sealed with a stopper and then incubated for 6 min at room temperature. Three separate tests were conducted, with each sample being evaluated three times.

2.7.3. FRAP Method

In order to assess the antioxidant capacity of silymarin, bio-ferment, and extract, the FRAP method was used [35]. The analyses were performed on the Thermo Scientific GENESYS 50 apparatus at the wavelength $\lambda = 593$ nm. Trolox (6-hydroxy-2,5,7,8-tetramethylchroman-2-carboxylic acid) was used as a reference substance. The antioxidant activity was expressed as mmol Trolox/L of appropriate cosmetic raw material, based on the resulting calibration curve $y = 0.6747x + 0.0218$ ($R^2 = 0.998$).

First, a 1% ethanolic solution of silymarin was prepared. To prepare the reagent, 25 mL of acetate buffer (0.3 M, pH = 3.6) was mixed with 2.5 mL of 2,4,6-tripyridyl-s-triazine solution (0.01 M TPTZ) in HCl (0.04 M HCl) and with 2.5 mL of FeCl₃ solution (0.02 M). The antioxidant activity of the prepared solution and the obtained bio-ferment (B) and extract (E) was measured as follows: 2.90 mL solution of TPTZ with an absorbance of about 1.000 ± 0.020 at $\lambda = 593$ nm was placed in the tube, and 0.1 mL of the ethanolic solution of silymarin or obtained cosmetic raw materials was added. Blank samples without antioxidants were prepared in the same way. The tubes were wrapped in aluminum foil, sealed with a stopper, and then incubated for 15 min at room temperature. Three independent experiments were performed, and each sample was analyzed three times.

2.7.4. Total Polyphenol Content (TPC)

To quantify the overall polyphenol content of silymarin, bio-ferment, and extract, the Folin-Ciocalteu method was used [34]. The analyses were conducted on the Thermo Scientific GENESYS 50 apparatus at the wavelength $\lambda = 750$ nm. Gallic acid (GA) served as the reference material. The total polyphenol content was expressed as mmol GA/L of appropriate cosmetic raw material, based on the resulting calibration curve of gallic acid: $y = 0.0075x$ ($R^2 = 0.997$).

First, a 1% ethanolic solution of silymarin was prepared. The total polyphenol content of the prepared solution and the obtained bioferment and extract were measured in the following manner: 2 mL of Folin-Ciocalteu reagent, 100 μ L of appropriate cosmetic raw material, and 1 mL of aqueous sodium carbonate (saturated solution) were introduced into 10 mL flasks. The contents of the flasks were made up to the mark with distilled water, the flasks were closed tightly with a stopper and incubated at room temperature for 15 min, and the absorbance of the test solutions was measured using a spectrophotometer at a wavelength of $\lambda = 750$ nm. Control samples devoid of antioxidants were generated using the same methodology. Three independent experiments were performed, and each sample was analyzed three times.

The total polyphenol content was calculated according to the following formula:

$$\text{TPC} = \frac{[(C_{\text{FAt.s.}} - C_{\text{FAr.s.}}) \cdot V_s]}{V_{\text{c.r.m.}}} \cdot 100\% \quad (1)$$

where:

TPC—Total polyphenol content by F–C method (mg/L);

$C_{\text{FAt.s.}}$ —concentration of phenolic acids in tested sample (mg/L);

$C_{\text{FAr.s.}}$ —concentration of phenolic acids in the reference sample (mg/L);

V_s —total volume of solution introduced into volumetric flasks (L);

$V_{\text{c.r.m.}}$ —volume of appropriate cosmetic raw material introduced into volumetric flasks (L).

2.7.5. Chelating Activity of Fe^{2+}

The colorimetric assay to investigate the Fe^{2+} chelating ability of bio-ferment and extract used ferrozine [36]. Metal ion chelation plays a strong role in preventing the generation of reactive oxygen species [37]. The calibration curve for Fe^{2+} ions was prepared using aqueous solutions of FeSO_4 . First, an initial FeSO_4 solution with an Fe^{2+} concentration of 0.53 mmol/L was prepared. Next, a ferrozine initial solution with a concentration of 3.2 mmol/L was prepared. Then 1 mL of the initial FeSO_4 solution (final Fe concentrations of 3, 1.2, 0.6, and 0.3 mg/L) and 1 mL of ferrozine were introduced into 10, 25, 50, and 100 mL volumetric flasks, the contents of the flasks were made up to the mark with distilled water, the flasks were closed tightly with a stopper and incubated at room temperature for 10 min, and then the absorbance of the test solutions was measured (using the Thermo Scientific GENESYS 50 apparatus at the wavelength $\lambda = 562$ nm), obtaining a calibration curve for Fe^{2+} ions ($y = 0.4888x + 0.0064$; $R^2 = 0.999$).

In the next stage, 1 mL of initial FeSO_4 solution, 0.1 mL of appropriate cosmetic raw material (or a 1% ethanolic solution of silymarin), and 1 mL of ferrozine were introduced into 10 mL volumetric flasks. The contents of the flasks were made up to the mark with distilled water, the flasks were closed tightly with a stopper and incubated at room temperature for 10 min, and then the absorbance of the test solutions was measured using a spectrophotometer at a wavelength of $\lambda = 562$ nm. Three independent experiments were performed, and each sample was analyzed three times.

The chelating activity of Fe^{2+} ions was calculated according to the following formula:

$$\text{ChA} = \frac{[(C_{\text{Fe}^{2+}\text{r.s.}} - C_{\text{Fe}^{2+}\text{t.s.}}) \cdot V_s]}{V_{\text{c.r.m.}}} \cdot 100\% \quad (2)$$

where:

ChA—chelating activity of Fe^{2+} (mg/L);

$C_{\text{Fe}^{2+}\text{r.s.}}$ —concentration of Fe^{2+} ions in the reference sample (mg/L);

$C_{\text{Fe}^{2+}\text{t.s.}}$ —concentration of Fe^{2+} ions in the tested sample (mg/L);

V_s —total volume of solution introduced into volumetric flasks (L);

$V_{\text{c.r.m.}}$ —volume of appropriate cosmetic raw material introduced into volumetric flasks (L).

2.7.6. Acidity

Acidity testing [38] of appropriate cosmetic raw materials was carried out by titration with NaOH solution and phenolphthalein as an indicator. In a ground conical flask, 10 mL of distilled water, 2 mL of the corresponding cosmetic raw material (i.e., bio-ferment, extract, or a 1% ethanolic solution of silymarin), and 3 drops of ethanolic solution of phenolphthalein were introduced. The flask was closed with a stopper, and its contents were mixed and then titrated with NaOH solution until the solution turned slightly pink. Blank analyses were performed in parallel.

The acidity (A) of the tested cosmetic raw materials was determined as the number of sodium hydroxides that are required to neutralize the test sample with the equivalent number of carboxyl groups (Kw) according to the following equation:

$$A = \frac{(V - V_0) \cdot N}{V_p} \cdot 40 \text{ or } = \frac{(V - V_0) \cdot N}{V_p} \quad (3)$$

where:

A—acidity (mmol COOH/L);

V—volume of NaOH solution (L);

V₀—volume of NaOH solution used for titration of the blank (L);

V_p—volume of NaOH solution used for titration of the sample of the corresponding cosmetic raw material (L);

C—concentration of NaOH solution (0.1 N).

2.8. The Skin Permeability of Hydrogels and Organogels and the Cumulative Mass of Active Compounds

The skin permeability for formulations (hydrogels and organogels containing silymarin, bio-ferment, and extract) of H-S, H-B, H-E, O-S, O-B, and O-E was assessed in Franz diffusion cells (Phoenix DB-6, ABL&E-JASCO, Wien, Austria) that consisted of a 1 mL donor chamber and a 10 mL acceptor chamber. The acceptor chamber, equipped with a magnetic stirring bar, was filled with PBS solution at a pH of 7.4. The acceptor chamber was maintained at a constant temperature of 37 ± 0.5 °C. Prior to commencing the examination, Franz diffusion cells were allowed to equilibrate at 37 °C for 15 min. The study utilized porcine skin owing to its comparable permeability qualities to human skin. The skin originated from a nearby abattoir. A fresh portion of skin from the abdomen was washed several times with a solution of PBS. Skin with a thickness of 0.5 mm was cut with a dermatome, and then it was enveloped in aluminum foil and frozen at a temperature of −20 °C for a maximum of 3 months [32,39,40]. Before the study, the skin was thawed at room temperature for about 30 min, and then it was soaked in PBS solution for 15 min to hydrate it. Subsequently, the skin was affixed to Franz diffusion cells. The integrity of the skin was checked 1 h after its installation in the Franz diffusion chamber (SES GmbH Analyse System, Bechenheim, Germany). In order to achieve this objective, the measurement of skin impedance was conducted using a 4080 m LCR (Conrad Electronic, Bechenheim, Germany) operating in parallel mode at 120 Hz (kΩ error < 0.5%). To take the measurement, the tips of the probes were immersed in the donor and acceptor chambers filled with the PBS solution. The membranes have an electrical resistance that is more than 3 kΩ, which is equivalent to the resistance observed in normal human skin [34].

Formulations (H-S, H-B, H-E, O-S, O-B, and O-E) were positioned within the donor chamber. All donor chambers were closed with a plastic stopper to prevent excessive evaporation of the vehicle. The aforementioned tests were conducted for a duration of 24 h. A 0.5 mL portion of the solution in the acceptor chamber was taken at specified intervals (0.5, 1, 2, 3, 4, 5, 8, and 24 h), and then augmented with a new aliquot of buffer at an identical pH [35]. The samples underwent analysis using high-performance liquid chromatography (HPLC). Upon the conclusion of the permeation experiment, the skin was extracted to estimate the amount of silymarin accumulated in the skin.

It was assessed whether the active substance contained in formulations penetrated the skin. Active substance contained in H-S, H-B, H-E, O-S, O-B, and O-E formulations penetrating the acceptor chamber was determined via HPLC [34]. The experiment was conducted with a Franz diffusion chamber, in which the donor phase consisted of the formulations tested. The acceptor phase consisted of a PBS solution, because it corresponds to systemic conditions, exhibits isotonic properties, and resembles conditions prevailing in the deeper layers of the skin [40]. After 24 h of the experiment, it was observed that the active substance contained in formulation penetrated the skin.

2.9. High-Performance Liquid Chromatography (HPLC)

The level of silybin and taxifolin in the acceptor fluid and accumulation in the skin via Knauer liquid chromatography system (Berlin, Germany) were assessed. The HPLC system consists of a Smartline model 2600 UV detector, model 1050 pump, and a Smartline model 3950 autosampler with ClarityChrom 2009 software. The detector was operated at 280 nm. A 125 × 4 mm chromatographic column filled with Hyperisil ODS (C18), with a particle size of 5 µm, was used. The mobile phase consisted of 0.05 M potassium dihydrogen phosphate–acetonitrile (60/40 *v/v*) with a flow rate of 1 mL/min. The column temperature was set to 25 °C, and the injection volume was 20 µL. Routine calculations of silybin and taxifolin content in the analyzed samples were performed by comparing the peak area with that of the reference. The chromatographic peaks of silybin and taxifolin were confirmed by comparing their retention times and UV spectra with those of reference compounds. Data from the literature show that the main components contained in the obtained bio-ferment and extract (silybin and taxifolin), which are part of the silymarin complex, show maximum absorption between 280 and 290 nm [41]. Therefore, HPLC analyses were conducted at 280 nm. The choice of the C18 column was based on data from the literature [41]. In addition, our preliminary studies have shown that the use of a C18 column allows for adequate separation of the analyzed compounds.

2.10. Elemental Analysis

A Thermo Scientific™ FLASH 2000 CHNS/O Analyzer (Waltham, MA, USA) was used to perform the CHNS/O elemental analysis. For CHNS mode analysis, formulations were weighed in tin crucibles (2.4–2.8 mg), and for oxygen mode analysis, they were weighed in silver crucibles (1.2–1.6 mg), with an accuracy of 0.000001 g. The device was calibrated in CHNS mode using L-cysteine, L-methionine, sulfanilamide, and 2,5-(Bis(5-tert-butyl-2-benzoxazol-2-yl) thiophene (BBOT) as standards. In the oxygen mode, benzoic acid and acetanilide were used [28,42].

2.11. Biodegradation of Formulations by Bacterial Cultures

2.11.1. The Test Medium and Origin of Samples of Active Sludge

The following solutions (per liter) were added to the test medium to prepare it: a volume of 10 mL of solution A (adjusted to pH of 7.4): 8.50 g of KH_2PO_4 , 21.75 g of K_2HPO_4 , 0.50 g of NH_4Cl , and 33.40 g of $\text{Na}_2\text{HPO}_4 \cdot 2\text{H}_2\text{O}$; a volume of 1 mL of solution B: 22.50 g of $\text{MgSO}_4 \cdot 7\text{H}_2\text{O}$; 1 mL of solution C: 36.40 g of $\text{CaCl}_2 \cdot 2\text{H}_2\text{O}$; and 1 mL of solution D: 0.25 g of $\text{FeCl}_3 \cdot 6\text{H}_2\text{O}$.

First, samples of active sludge were taken from the aeration chamber of the Pomorzany sewage treatment plant in Szczecin. After that, the samples were aerated and kept until needed. A microbiological test (Schulke Mikrocount Duo) was used to determine the level of active sludge concentration suspensions in order to calculate the total number of microorganisms (CFU/1 mL of active sludge). A microbiological test containing medium and TTC agar with Tergitol-7 (triphenyl tetrazolium chloride) was immersed in active sludge for 10 s. The amount of bacteria was determined by comparing the test's appearance to that of a standard test after 96 h at room temperature (Figure S1) [26].

The Microbial Challenge Test was executed in compliance with the prescribed instructions provided in [35]. Schulke+ mikrocount® duo dipslides, which have two agar

surfaces—the pink surface supporting fungal and yeast growth and the yellow surface supporting the growth of bacteria, such as *Staphylococcus species* or *Escherichia coli*—were used to conduct the microbiological challenge test. The test sample of activated sludge was submerged in the yellow surface of the agar. To allow for the best possible level of bacterial growth, the slide was then sealed and left for 72 h. Every measurement was conducted at a room temperature of 25 ± 1 °C and relative humidity of 33%. The density of the colony formed on the nutrient plate is determined using the colony density charts specified by Schulke. Microbial growth was seen in the 10 activated sludge samples that were analyzed after 72 h. The evaluated activated sludge samples contained 10^6 CFU/mL of activated sludge in relation to the colony density.

In addition, the total number of microorganisms was determined on 1 mL of activated sludge (0.95×10^5 CFU/mL) by the experimental method in agar medium. For bacterial cultivation, Merck Millipore's lactose Tergitol 7 TTC agar medium was used. Petri dishes with a diameter of 90 mm were filled with the medium (20 mL). One milliliter of activated sludge (diluted 1000 times in PBS) was added to the medium after it had solidified. The inoculum was dispersed uniformly over the medium's surface. To allow for the best possible level of bacterial growth, the slide was then sealed and left for 72 h. Every measurement was conducted at a room temperature of 37 ± 1 °C. Final analyses were conducted using the data obtained after 72 h. Following this, a range of 95 to 99 bacterial colonies was determined. The studies showed that the density of the bacterial cultures ranged from 0.95 to 0.99×10^6 CFU/mL.

2.11.2. Method for Determining the Potential for Aerobic Biodegradation of Formulations

The only sources of carbon and energy were H-B, H-E, H-S, O-B, O-E, O-S, and SDS (sodium dodecyl sulfate as reference compound) formulations with organic carbon concentration of 40 mg/L, which were tested in duplicate, and the results are presented as mean + SD. Two tests were conducted independently (in two measuring vessels).

Figure 2 presents the arrangement of the test vessels (1.1, 1.2, 1.3, 1.4, and 1.5) and the placement of a magnetic stirrer (1.6) connected with tubes. The test apparatus was aerated by air (I) passing through carbon dioxide (CO₂) absorbers (B and C). The velocity of the air was regulated by a valve, which was routed to a carbon dioxide absorber (1.1), followed by a CO₂ indicator (1.2), with the intention of indicating the presence of carbon dioxide in the air via turbidity. A total of 250 mL of the test medium, 25 mg of dried active sludge, and formulations corresponding to 40 mg/L of organic carbon were deposited in test vessel 1.3. The concentrations of the starting formulations were 69.78 mg for H-B, 70.37 mg for H-E, 71.53 mg for H-S, 13.66 mg for O-B, 13.68 mg O-E, 13.87 mg for O-S, and 84.11 mg for SDS, respectively.

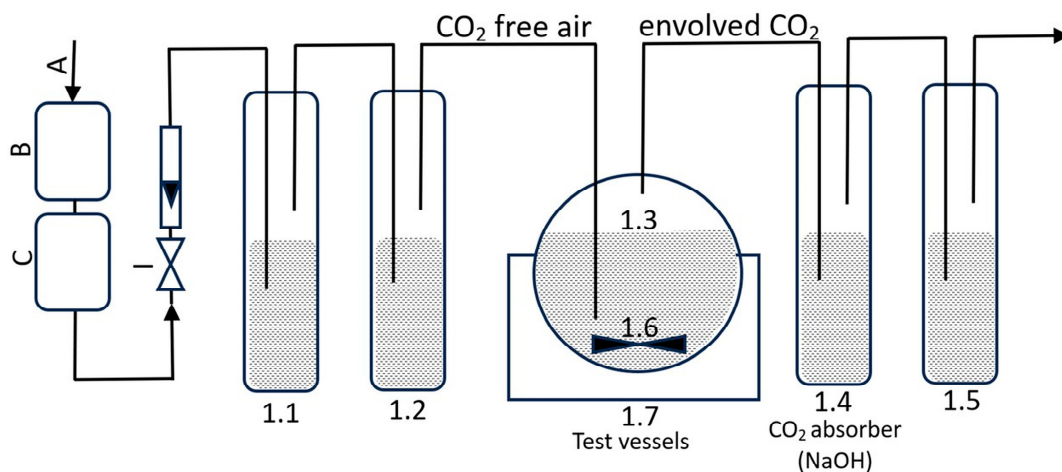
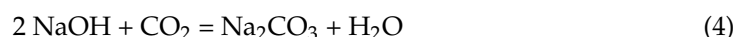
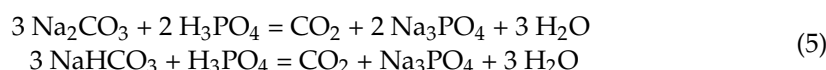


Figure 2. The carbon dioxide measurement method.

The formulation's capacity for biodegradation resulted in the production of CO₂ in vessel 1.3, which reacted with sodium hydroxide (NaOH) to produce sodium carbonate (Na₂CO₃):



To determine the CO₂ concentration in vessel 1.3, 10 mL of the solution from vessel 1.4 was moved into a 25 mL volumetric flask. Deionized water was added to the flask until the designated maximum level was reached. Next, the sample was analyzed (twice) with total organic carbon analyzer (TOC-LCSH/CSN Shimadzu Corporation) as follows:



The test sample comprises carbonates (Na₂CO₃) and acidic carbonates (NaHCO₃) that were acidified with orthophosphoric acid (H₃PO₄) to achieve a pH of 2–3. Na₂CO₃ and NaHCO₃ acidified with H₃PO₄ are converted to CO₂. First, sodium bicarbonate (NaHCO₃) and sodium carbonate (Na₂CO₃) calibration curves were created. In order to achieve this, 4.415 g of Na₂CO₃ (which had been dried for two hours at 285 °C in a muffle furnace) and 3.500 g of NaHCO₃ (which had been dried for two hours over silica gel) were added to a 1000 mL flask. The flask was then filled with deionized water (previously boiled). From the starting solution thus prepared, dilutions of sodium carbonate and sodium bicarbonate were prepared in the concentration range of 0–100 mg/L inorganic carbon (IC), and a calibration curve was prepared. The volume of the dispensed sample was 50 µL. Utilizing the calibration curve ($y = 4.1187x + 7.1718$; $R^2 = 0.999$), the inorganic carbon (IC) content in the test specimens was determined.

The carbon dioxide measuring apparatus as seen in Figure 2 was made up of the following parts:

- I: air with an aeration rate of 50–100 mL/min, used to aerate the all test systems;
 - B and C: CO₂ absorber (potassium hydroxide);
 - 1.1: CO₂ absorber (potassium hydroxide at 5 mol/L concentration);
 - 1.2: CO₂ indication (barium hydroxide at 0.01 mol/L concentration);
 - 1.3: 500 mL capacity test vessels stirred with magnetic stirrer (1.6);
 - 1.4: CO₂ absorber (sodium hydroxide at 0.05 mol/L concentration);
 - 1.5: O₂ absorber (distilled water);
 - 1.7: container filled with distilled water, inside which test vessels with a 500 mL capacity were placed;
 - 1.8: cryostat that precisely sets the temperature of the distilled water in the container.
- Incubation was carried out at 23 ± 0.5 °C for 28 days.

The biodegradation degree of the test formulations was determined according to the following formula:

$$\%B = \frac{[C_{ICi} \cdot V_0 + \sum_{i=1}^n (C_{ICi+1} + C_{ICi}) \cdot (V_0 - i \cdot V_p)] \cdot R}{m \cdot U} \cdot 100\% \quad (6)$$

where:

- %B—degree of biodegradation;
- C_{IC}—concentration of inorganic carbon in test vessel 1.4, obtained by TOC analysis of the test sample corrected by blank (mg/L);
- R—dilution of the sample collected from test vessel 1.4 (2.5);
- V₀—initial volume of NaOH solution in test vessel 1.4 (0.25 L);
- i—sample number;
- V_p—volume of sample taken from test vessel 1.4 (0.01 L);
- m—mass of test formulation injected into test vessel 1.3 (mg);
- U—the proportion of carbon in the test formulation introduced into test vessel 1.3.

2.12. Statistical Analysis

Results are displayed as the mean \pm standard deviation (SD). A one-way analysis of variance (ANOVA) was used. As for the cumulative mass after 24 h of permeation and the cumulative mass in the skin, the significance of differences between individual groups was evaluated with the Tukey's test ($\alpha < 0.05$). A cluster analysis was conducted to determine similarities between all compounds tested and all vehicles, considering all time points. On this basis, we presented groups of compounds with a similar permeation. Statistical computations were performed using *Statistica 13 PL* software 7 (StatSoft, Kraków, Poland).

3. Results

3.1. Contact Angle

Figure 1a–h display images of water droplets on the surface of the obtained formulations. The H (c.a._{av.} $12.1^\circ \pm 2.0$), H-B (c.a._{av.} $15.3^\circ \pm 2.1$), and H-E (c.a._{av.} $9.9^\circ \pm 1.9$) gel formulations had the most hydrophilic surface, which is strongly due to the active substance (bio-ferment and extract) used and the vehicle from which the formulations were made. The H-S (c.a._{av.} $42.3^\circ \pm 2.1$) and O-S (c.a._{av.} $36.4^\circ \pm 2.0$) formulations had the most hydrophobic surface, which is due to the silymarin, which is characterized by a partition coefficient (logP) of 1.8 [43]. A smaller contact angle indicates a higher level of hydrophilicity, and the higher one has a lower level of hydrophilicity [44].

The measured contact angle was determined to be $26.2^\circ \pm 2.1$ for the pure organogel (O). Typically, with the addition of the active ingredient (i.e., bio-ferment and extract), the contact angle for the O-B (c.a._{av.} $25.1^\circ \pm 2.1$) and O-E (c.a._{av.} $10.4^\circ \pm 1.8$) formulations decreased. This is most likely due to the increased hydrophilicity of the active substances contained in these cosmetic raw materials [37].

3.2. Activity, Fe^{2+} Chelating Activity, Antioxidant Activity, and Total Polyphenol Content

Table 2 displays the outcomes for the activity of a 1% ethanolic solution of bio-ferment (B), extract (E), and silymarin (S).

Table 2. The results for the activity of bio-ferment (B), extract (E), and silymarin (S).

Cosmetic Raw Material	Antioxidant Activity				Fe^{2+} Chelating Activity	Acidity/Lactic Acid Content
	DPPH	ABTS	FRAP	TPC	ChA	A
	mmol Trolox/L c.r.m.	mmol Trolox/L c.r.m.	mmol FeSO ₄ /L c.r.m.	mmol GA/L c.r.m.	mmol Fe/L c.r.m.	mmol COOH/L c.r.m./g
Extract	0.91 \pm 0.2 a	0.10 \pm 0.02 a	0.52 \pm 0.12 a	0.61 \pm 0.04 a	0.01 \pm 0.00 a,b	not tested
Bio-ferment	1.19 \pm 0.2 a	0.20 \pm 0.01 b	1.34 \pm 0.19 b	0.92 \pm 0.05 a,b	0.05 \pm 0.01 b	215.00 \pm 1.00/5.60
Silymarin	1.14 \pm 0.3 a	0.11 \pm 0.02 a	0.99 \pm 0.19 b	0.76 \pm 0.09 a	na	not tested

Mean \pm SD ($n = 9$); a, b—different letters: the investigated formulations exhibit substantial variations in values, as seen by the present findings; na—not active.

Table 2 shows the antioxidant activity (via a DPPH radical scavenging assay and the ABST method), total polyphenol content (via the Folin–Ciocalteu method), Fe^{2+} chelating activity, and acidity of a 1% ethanolic solution of silymarin (S), bio-ferment (B), and extract (E). The investigation of the DPPH radical scavenging capability of the 1% ethanolic solution of silymarin (S), bio-ferment (B), and extract (E) showed that the E, B, and S were characterized by DPPH radical scavenging degrees of 0.91 mmol Trolox/L c.r.m. \pm 0.2, 1.19 mmol Trolox/L c.r.m. \pm 0.2, and 1.14 mmol Trolox/L c.r.m. \pm 0.3, respectively. The test results, presented in Table 2, show that the obtained cosmetic raw materials (B, E) and the solution of silymarin (S) exhibited antioxidant properties, as evaluated via the ABTS, FRAP, and Folin–Ciocalteu methods. The antioxidant activity (decided by the ABTS method) of the E, B, and S showed that the bio-ferment had the highest antioxidant activity (0.20 mmol Trolox/L c.r.m. \pm 0.01). A 50% decrease in antioxidant activity was noted for the extract and solution of silymarin. The antioxidant activity determined by the FRAP method showed that the bio-ferment had the highest antioxidant activity (1.34 mmol FeSO₄/L c.r.m. \pm 0.19). A lower level of activity was ob-

served for the extract ($0.52 \text{ mmol FeSO}_4/\text{L c.r.m.} \pm 0.12$) and the solution of silymarin ($0.99 \text{ mmol FeSO}_4/\text{L c.r.m.} \pm 0.19$). Studies of the chelating activity of Fe^{2+} ions in the ferrozine test showed that the chelating activity of the tested bio-ferments' reduction potential is $0.05 \text{ mmol Fe/L c.r.m.} \pm 0.01$ (acidity $A = 215.00 \text{ mmol COOH/L c.r.m.} \pm 1.00$), while in the case of the extract, the ChA value is five times lower ($0.01 \text{ mmol Fe/L c.r.m.} \pm 0.00$), with the silymarin solution showing no ChA—Table 2.

3.3. Penetration Studies

The total mass of silybin and taxifolin in the acceptor fluid at all time points is depicted in Figures 3 and 4.

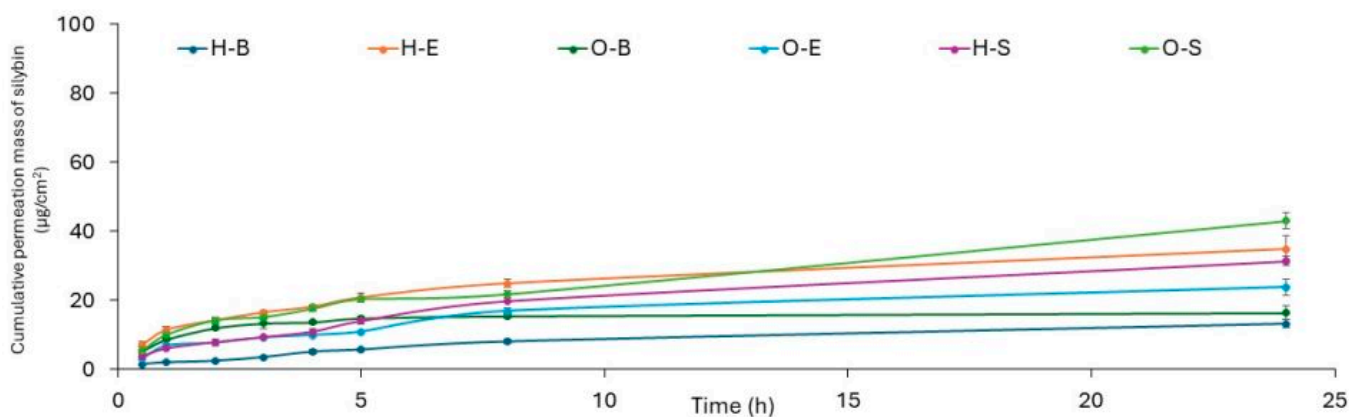


Figure 3. Time course of the cumulative mass of silybin during the 24 h penetration period (mean \pm SD, $n = 3$).

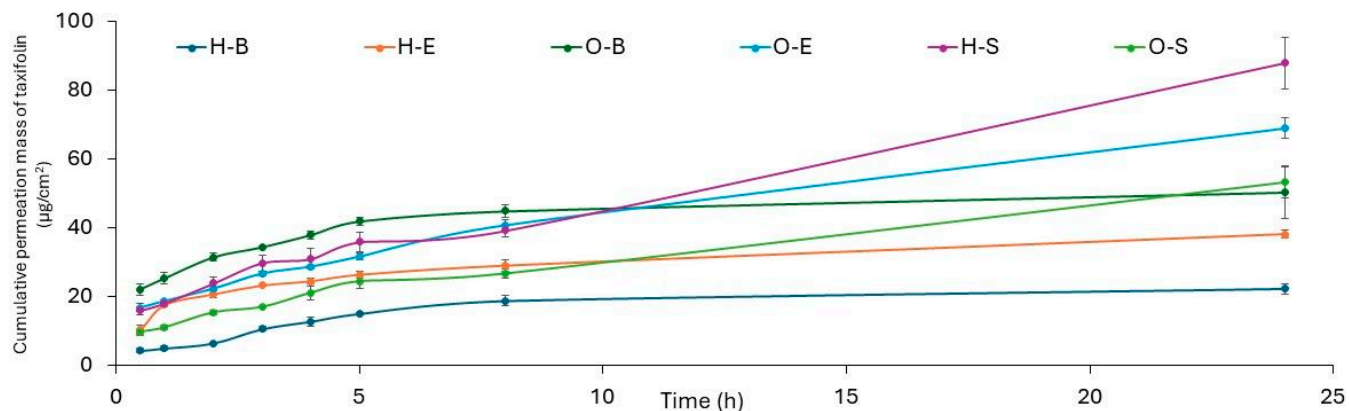


Figure 4. Time course of the cumulative mass of taxifolin during the 24 h penetration period (mean \pm SD, $n = 3$).

In contrast, the silybin and taxifolin content in the acceptor fluid gathered across the 24 h penetration period is summarized in Table 3.

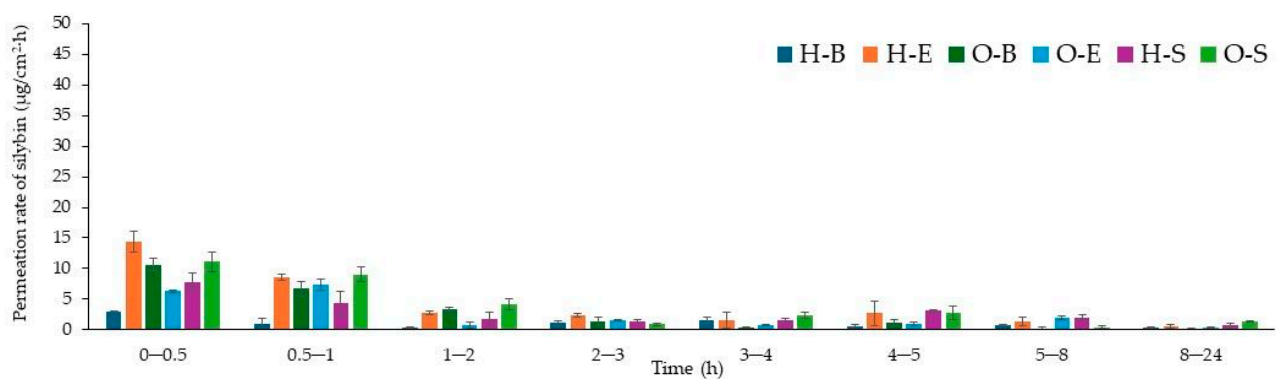
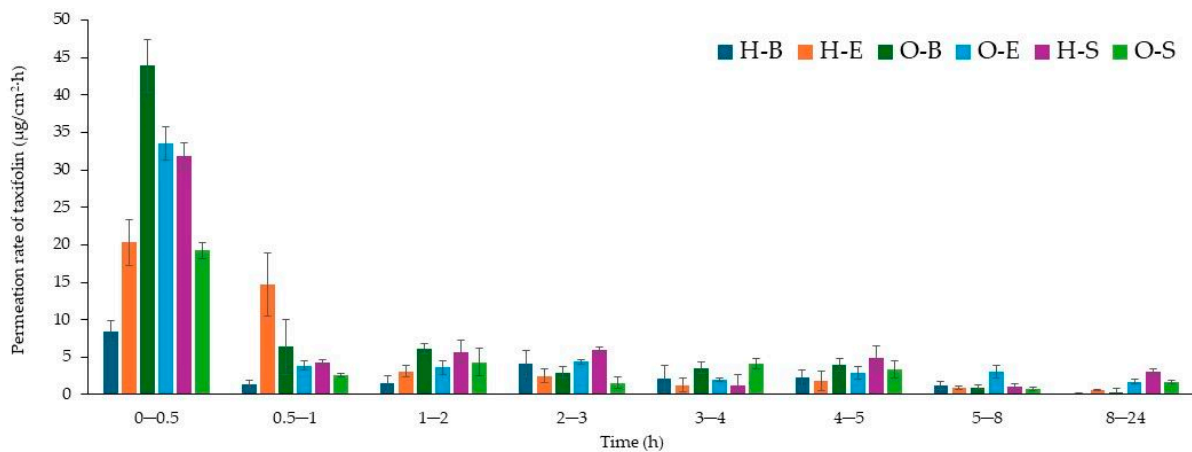
After 24 h of penetration, the cumulative mass of silybin had the following order: $\text{H-S} > \text{H-E} > \text{O-S} > \text{O-E} > \text{O-B}$ and H-B . Among the tested preparations, H-S exhibited the highest significant level of penetration of silybin, with a gradual infiltration of $43.107 \pm 2.401 \text{ } \mu\text{g}/\text{cm}^2$. However, after 24 h of permeation, the cumulative mass of taxifolin had the following order: $\text{H-S} > \text{O-E} > \text{O-S} > \text{O-B} > \text{O-B}, \text{H-E},$ and H-B . Among the tested preparations, H-S also exhibited the highest significant level of infiltration of taxifolin, with a cumulative permeation of $87.739 \pm 7.457 \text{ } \mu\text{g}/\text{cm}^2$. It was observed that both silymarin and taxifolin were released the fastest in the first hour of the test out of all the analyzed formulations (Table 3, Figures 3, 4 and S2).

Table 3. Cumulated mass for silybin and taxifolin after 24 h penetration with various preparations.

Formulation	Silybin	Taxifolin
	Cumulative Penetration Mass ($\mu\text{g}/\text{cm}^2$)	
H-B	13.283 ± 1.072 a	22.136 ± 1.431 a
H-E	34.851 ± 3965 d	38.025 ± 1.218 b
H-S	43.107 ± 2.401 e	87.739 ± 7.457 e
O-B	16.410 ± 2.070 ab	50.213 ± 7.586 bc
O-E	23.838 ± 2.213 bc	68.852 ± 3.132 d
O-S	31.385 ± 1.416 cd	53.082 ± 4.51 c

Distinct letters denote substantial disparities among the preparations of the analysis; $\alpha = 0.05$, mean \pm SD, $n = 3$. The statistically significant difference was estimated via ANOVA using the Tukey's test.

The penetration rate of silybin and taxifolin during the 24 h penetration test is shown in Figures 5 and 6.

**Figure 5.** The penetration rate of silybin during the 24 h penetration period (mean \pm SD, $n = 3$).**Figure 6.** The penetration rate of taxifolin during the 24 h penetration period (mean \pm SD, $n = 3$).

The main components of the silymarin complex, such as silybin and taxifolin, contained in the extract and bio-ferment are shown in Table 4.

Table 4. Values of compounds of silymarin in bio-ferment and extract of *S. marianum*.

Cosmetic Raw Material	Silybin	Taxifolin
	mg/100 mL	
Bio-ferment	5.915 ± 0.238 b	49.357 ± 1.942 b
Extract	2.099 ± 0.079 a	22.550 ± 0.232 a

Mean (\pm standard deviation), ($n = 3$); distinctive letters denote substantial disparities between bio-ferment and extract; $\alpha = 0.05$. The statistically significant difference was estimated via ANOVA using the Tukey's test.

The bio-ferment from *S. marianum* contained a significantly higher amount of the analyzed ingredients compared to the extract from this plant. The content of silybin was almost three times greater in magnitude than the bio-ferment and amounted to 5.915 ± 0.238 mg/mL, while that of taxifolin was almost twice as high at 49.357 ± 1.942 mg/mL compared with the extract (Table 4).

3.4. Elemental Analysis of Formulations

Prior to commencing the biodegradation trials, the organic carbon (C) content was confirmed through an elemental analysis. The results for the carbon content of the tested H-B, H-E, H-S, O-B, O-E, and O-S formulations were, respectively, 69.78%, 70.37%, 71.53%, 13.66%, 13.68%, and 13.87%.

3.5. Biodegradation Studies

Table 5 shows the hydrogel and organogel formulations' biodegradation by bacterial cultures.

Table 5. Formulations' biodegradation by bacterial cultures.

Time (Days)	* Biodegradation after 28 Days					
	H-B	H-E	H-S	O-B	O-E	O-S
	(%)					
0	0 ± 0	0 ± 0	0 ± 0	0 ± 0	0 ± 0	0 ± 0
1	2 ± 1	4 ± 2	2 ± 3	2 ± 1	2 ± 2	2 ± 1
2	3 ± 2	8 ± 1	3 ± 4	4 ± 2	3 ± 2	4 ± 1
6	4 ± 4	13 ± 3	4 ± 2	6 ± 3	4 ± 1	6 ± 1
7	5 ± 3	15 ± 2	5 ± 3	9 ± 2	6 ± 5	9 ± 2
9	11 ± 4	17 ± 3	10 ± 1	14 ± 3	10 ± 3	14 ± 2
13	29 ± 2	19 ± 2	29 ± 1	19 ± 3	28 ± 2	19 ± 2
14	36 ± 1	18 ± 4	36 ± 1	33 ± 4	36 ± 4	33 ± 3
16	38 ± 2	22 ± 5	38 ± 3	38 ± 3	38 ± 4	38 ± 2
17	42 ± 3	23 ± 4	42 ± 4	44 ± 3	39 ± 6	44 ± 3
22	44 ± 1	23 ± 2	44 ± 2	46 ± 2	41 ± 3	46 ± 3
23	47 ± 5	26 ± 3	44 ± 4	49 ± 4	41 ± 6	49 ± 5
27	47 ± 4	33 ± 3	45 ± 5	54 ± 2	42 ± 5	54 ± 4
28	47 ± 3	35 ± 3	45 ± 4	60 ± 4	43 ± 4	60 ± 2
** Qualitative assessment of aerobic biodegradability	●	●	●	●	●	●

* Mean ± SD ($n = 6$). For each prepared formulation, two independent experiments were performed, during which the collected samples were analyzed three times. ** Categories: "●"—Readily biodegradable with degree of biodegradation $\geq 60\%$; "●"—Poorly biodegradable with degree of biodegradation below 60%.

After 28 days, the highest percentage of biodegradation was $60\% \pm 4$ (O-B) and $60\% \pm 2$ (O-S), which classifies these formulations as readily degradable. Following 28 days of the experiment, poor biodegradation susceptibility was reported in four formulations: H-B ($46\% \pm 6$), H-E ($35\% \pm 5$), H-S ($45\% \pm 4$), and H-E ($43\% \pm 4$). It has been shown that the type of cosmetic vehicle has a significant impact on the biodegradation of the formulations. Here is how the kind of vehicle affects biodegradation: (1) The easily biodegradable O-B and O-S formulations showed high levels of biodegradation after 28 days. This suggests that organogels based on biodegradable soy lecithin and Pluronic P127 containing bio-ferment and silymarin are readily biodegradable [45]. The presence of biodegradable components in these formulations likely enhances their susceptibility to microbial degradation. The type

of vehicles and type of cosmetic raw material (bio-ferment and pure silymarin) may make them more appealing to the biodegrading microorganisms, leading to higher degradation rates. (2) The poorly biodegradable H-B, H-E, H-S, and O-E formulations exhibited lower levels of biodegradation (ranging from $35\% \pm 3$ to $46\% \pm 3$) after 28 days. Despite the presence of biodegradable components in the O-E organogel vehicle, this formulation showed a reduced susceptibility to biodegradation. Specific components in the H-B, H-E, and H-S hydrogel vehicles may make them less accessible or less favorable to biodegrading microorganisms—Table 5 [46].

The half-life of formulations by bacterial cultures is shown in Table 6.

Table 6. The half-life of formulations by bacterial cultures.

The Half-Life of the Analyzed Formulations					
H-B	H-E	H-S	O-B	O-E	O-S
(h/Days)					
733/31	949/40	742/31	556/23	777/32	556/23

The shortest half-life of the O-B and O-S formulations was 23 days. Furthermore, the H-B, H-E, H-S, and O-E formulations had a longer half-life than 23 days: H-B and H-S both had a half-life of 31 days, O-E had a half-life of 32 days, and H-E had a half-life of 40 days, as shown in Table 5.

The phases of the degradation of the formulations are shown in Table 7.

Table 7. The phases of degradation of formulations.

Compound Name	Phase of Degradation					
	Lag Phase		Degradation Phase		Plateau Phase	
	%	Day	%	Day	%	Day
H-B	0–5	0–7	5–41	7–17	41–46	17–28
H-E	0–4	0–6	4–32	6–27	32–35	27–28
H-S	0–5	0–7	5–41	7–17	41–45	17–28
O-B	0–6	0–6	6–54	6–27	54–60	27–28
O-E	0–4	0–6	4–39	6–17	39–43	17–28
O-S	0–6	0–6	6–54	6–27	54–60	27–28

The H-E, O-B, O-E, and O-S formulations reached 10% degradation after 6 days, while H-B and H-S took longer than 6 days (7 days), which may be related to the adaptation of microorganisms during the lag phase [28]. The degradation phase of H-B, H-S, and O-E is 17 days. In contrast, for three formulations, H-E, O-B, and O-S, the degradation phase is longer (27 days), as shown in Table 7, and Figures 7a–c and 8a–c.

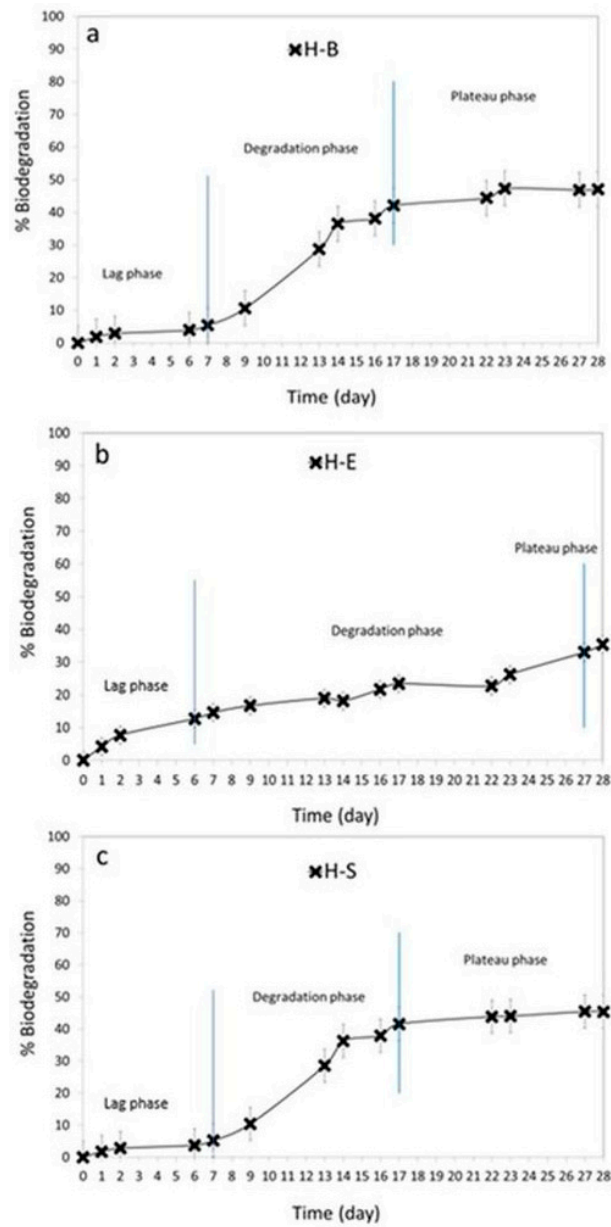


Figure 7. The phases of degradation of formulations: (a) H-B; (b) H-E; (c) H-S.

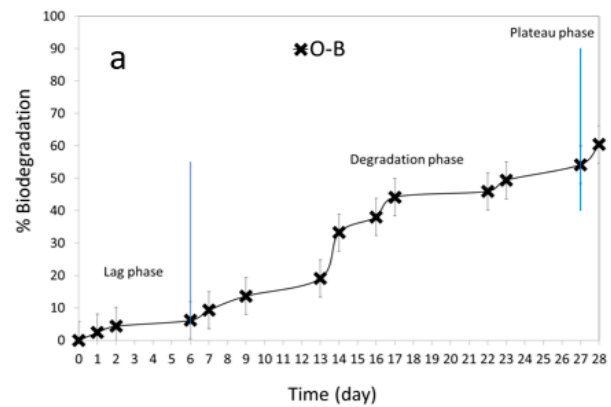


Figure 8. Cont.

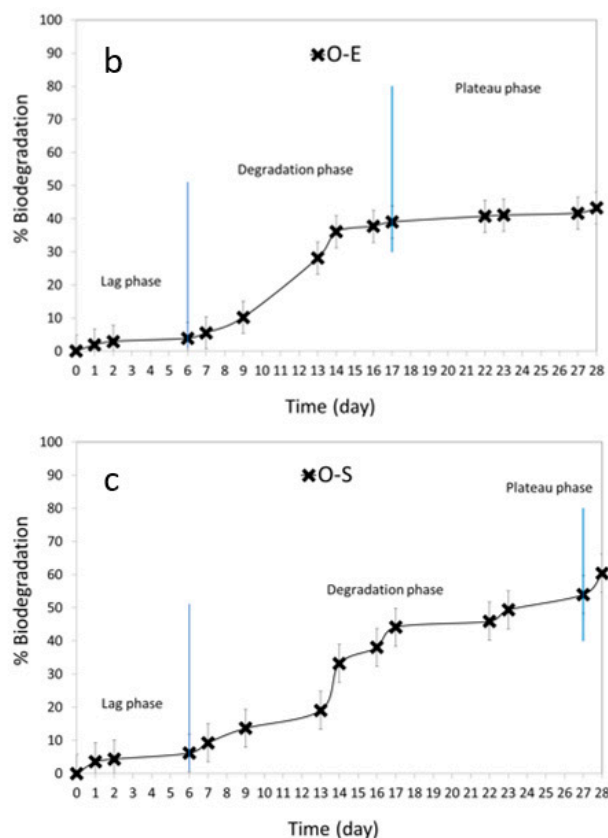


Figure 8. The phases of degradation of formulations: (a) O-B; (b) O-E; (c) O-S.

4. Discussion

In recent years, there has been an observed desire to explore innovative, efficient, and secure cosmetic formulations containing active ingredients with multiple effects. Additionally, cosmetic formulations containing mainly “natural” ingredients are perceived as safer compared to “synthetic” ingredients. One of the potential sources of valuable secondary metabolites used in cosmetology (as well as dermatology) are raw materials [33]. Extracts obtained from plant materials and fermented raw materials (i.e., innovative bio-ferments) are characterized by their antioxidant, anti-inflammatory, and anti-aging effects [40,47].

The fermentation of milk thistle using organic molasses and a mixture of *Lactobacillus* strains showed that the bacterial strains can produce lactic acid (in an amount of 5.60 g), as evidenced by our acidity (215.00 ± 1.00 mmol COOH/L) tests of the obtained bio-ferment (Table 2) and studies by other authors [48]. Our study showed that the bio-ferment showed the highest antioxidant activity via the DPPH, ABTS, and FRAP methods, the highest polyphenol content (via the Folin–Ciocalteu method), and higher chelating activity of Fe^{2+} ions (Table 2). The high antioxidant activity indicates that lactic fermentation increases the antioxidant activity of the fermented raw material. Studies by other authors have shown that fermenting plant raw materials in the presence of a carbon and energy source (for example, sucrose) increases lactic acid production [49]. The antioxidant activity of the extract and bio-ferment was evaluated via the DPPH method, as well as by linoleic acid and tyrosinase inhibition. The results showed that the bio-ferment showed higher linoleic acid inhibition activity, which affects skin pigmentation, so the bio-ferments were also credited with skin-tone-equalizing properties. On the other hand, the tyrosinase inhibition test showed the best results against the bio-ferment, proving that the obtained cosmetic raw material plays an important role in inhibiting melanin production. Antioxidants contained in fermented cosmetic raw materials are good tyrosinase inhibitors [6,50–52].

However, for active compounds contained in the obtained cosmetic raw materials to have a beneficial effect on the skin, they must reach the deeper layers of the skin. Therefore,

assessing the penetration of active compounds through the skin is an important element in modeling cosmetic formulations [53]. The penetration degree of active substances may be different, depending on the compounds' physical and chemical properties as well as the vehicle used [54]. The primary impediment that restricts the permeation of active compounds into the skin is the *stratum corneum* (SC), which serves to prevent excessive transdermal water loss as well as the ingress of germs and chemical substances [33,55]. The SC is a thin membrane consisting primarily of cornified epidermal cells, while the main components are lipids, namely ceramides, cholesterol and its esters, and fatty acids [56]. The extracts obtained from plant materials and fermented raw materials (i.e., innovative bio-ferments) can play an important role (due to the presence of active substances—mainly polyphenols and lactic acid produced during fermentation by lactic bacteria) in the proper hydration of the epidermis as well as the inflammation of the epidermis and underlying layers. The evaluation of the transdermal absorption of active compounds is an important element in preparing cosmetic and dermatological formulations [57].

The *in vitro* penetration was calculated in our investigation of extracts of *S. marianum*, the bio-ferment of *S. marianum*, and silymarin from various gel formulations (hydrogels and organogels). Two analyzed silymarin components, such as taxifolin and silybin, penetrated the skin from all the analyzed formulations (H-B, H-E, H-S, O-B, O-E, and O-S). Silybin and taxifolin, which penetrate into the deeper layers of the skin, can have a very beneficial effect not only on the surface but also in the deeper layers of the skin. Our research has shown that both the plant extract and bio-ferment of *S. marianum* can be highly active ingredients of biodegradable cosmetic (and even dermatological) formulations. Silybin and taxifolin contained in the silymarin complex may have primarily antioxidant, anti-aging, and anti-inflammatory effects [58–61].

The contact angle measurements can be used to assess the intermolecular attraction between the water molecules and the surface of the examined formulation. The stronger the attraction, the lower the contact angle value [38]. With the introduction of silymarin into the H-S and O-S formulations, the contact angle increased; i.e., the surface became more hydrophobic. For other formulations, by changing the type of cosmetic raw material (E and B), a decrease was observed in the contact angle values for the formulations with bio-ferment and extract.

Our permeability results, along with our biodegradation findings, provide a comprehensive understanding of both the environmental impact and cosmetic (dermatological) efficacy of the tested formulations. The type of vehicles and type of cosmetic raw material used directly impact the biodegradability of the formulations by bacterial cultures. Some vehicles enhance their biodegradability, making the compounds more easily degraded by microorganisms, while others reduce their biodegradability, making them persist longer in the environment. The appropriate type of cosmetical vehicle and the type of cosmetic raw material introduced likely play a crucial role in determining their biodegradation rates. The readily biodegradable formulations (O-S and O-B) exhibited high biodegradation rates, suggesting their susceptibility to microbial breakdown. Our permeability results can contribute to understanding their potential therapeutic efficacy. For instance, the O-S and O-B organogels with silymarin and bio-ferment demonstrated both high levels of biodegradability and significant permeation. This suggests that the organogel formulation, combined with bio-ferment or pure silymarin, may offer effective active substance delivery (with the desired level of antioxidant activity) and have a beneficial influence on the environment. Poorly biodegradable formulations (H-E, H-S, H-B, and O-E) showed lower biodegradation rates, indicating a reduced susceptibility to microbial breakdown.

Silymarin incorporated into suitable cosmetic vehicles (hydrogels or organogels) penetrates the dermal layer, which is the biggest obstacle to the transport of active substances. Interestingly, silymarin accumulates in the skin, which is also very beneficial because the collected active compounds in the skin can have a longer antioxidant effect, showing anti-aging effects.

5. Conclusions

In conclusion, our extended discussion reveals a nuanced understanding of how different cosmetic vehicles (hydrogels and organogels) influence the transdermal behavior of active substances (obtained from plant materials by extraction and lactic fermentation). Our research has implications for the development of cosmetic delivery systems for active substances tailored to specific therapeutic needs, considering the unique characteristics of each formulation. The integration of the permeability and antioxidant activity of these active substances (obtained by the extraction and fermentation of milk thistle) as well as the biodegradation of cosmetic formulations allow for a comprehensive evaluation of the environmental and cosmetic aspects of the tested preparations. This information is crucial for making informed decisions in terms of biodegradable cosmetic formulation design, considering both antioxidant activity and environmental sustainability.

Supplementary Materials: The following supporting information can be downloaded at: <https://www.mdpi.com/article/10.3390/app14010169/s1>, Figure S1: The appearance of the test obtained after immersion of the insert in the active active sludge—rights, the appearance of the reference test—left; Figure S2: The HPLC from bio-ferment of *S. marianum* (a) and extract of *S. marianum* (b), acceptor liquid after 24-h pentation (c) and pure silymarin used as a standard (d) A—taxifolin (RT = 1.32 min), B—silybin (RT = 1.83 min).

Author Contributions: Conceptualization, E.K. and R.S.; methodology, R.S., E.K., A.N. and Ł.K.; formal analysis, E.K., A.N., Ł.K., A.M.-S. and W.D.; investigation, E.K.; data curation, E.K.; writing—original draft preparation, E.K., R.S. and A.N.; writing—review and editing, R.P. and A.M.-S.; visualization, E.K.; supervision, A.B. and J.R. All authors have read and agreed to the published version of the manuscript.

Funding: This research received no external funding.

Institutional Review Board Statement: Not applicable.

Informed Consent Statement: Not applicable.

Data Availability Statement: Most of the data are provided in this work. Other data that support the findings of this study are available from the corresponding author upon reasonable request. The data are not publicly available due to privacy.

Acknowledgments: We would like to express our sincere gratitude to the “Pomorzany” Wastewater Treatment Plant in Szczecin for their invaluable collaboration and support in providing wastewater sludge for our research endeavors.

Conflicts of Interest: The authors declare no conflicts of interest.

References

1. Reihani, S.F.S.; Khosravi-Darani, K. Influencing Factors on Single-Cell Protein Production by Submerged Fermentation: A Review. *Electron. J. Biotechnol.* **2019**, *37*, 34–40. [[CrossRef](#)]
2. Hoang, H.T.; Moon, J.-Y.; Lee, Y.-C. Natural Antioxidants from Plant Extracts in Skincare Cosmetics: Recent Applications, Challenges and Perspectives. *Cosmetics* **2021**, *8*, 106. [[CrossRef](#)]
3. Lu, H.; Yang, K.; Zhan, L.; Lu, T.; Chen, X.; Cai, X.; Zhou, C.; Li, H.; Qian, L.; Lv, G.; et al. Optimization of Flavonoid Extraction in *Dendrobium Officinale* Leaves and Their Inhibitory Effects on Tyrosinase Activity. *Int. J. Anal. Chem.* **2019**, *2019*, 7849198. [[CrossRef](#)] [[PubMed](#)]
4. Ziemlewska, A.; Nizioł-Łukaszewska, Z.; Bujak, T.; Zagórska-Dziok, M.; Wójciak, M.; Sowa, I. Effect of Fermentation Time on the Content of Bioactive Compounds with Cosmetic and Dermatological Properties in Kombucha Yerba Mate Extracts. *Sci. Rep.* **2021**, *11*, 18792. [[CrossRef](#)] [[PubMed](#)]
5. Aguilar-Toalá, J.E.; Garcia-Varela, R.; Garcia, H.S.; Mata-Haro, V.; González-Córdova, A.F.; Vallejo-Cordoba, B.; Hernández-Mendoza, A. Postbiotics: An Evolving Term within the Functional Foods Field. *Trends Food Sci. Technol.* **2018**, *75*, 105–114. [[CrossRef](#)]
6. Majchrzak, W.; Motyl, I.; Śmigielski, K. Biological and Cosmetical Importance of Fermented Raw Materials: An Overview. *Molecules* **2022**, *27*, 4845. [[CrossRef](#)] [[PubMed](#)]
7. Pérez-Rivero, C.; López-Gómez, J.P. Unlocking the Potential of Fermentation in Cosmetics: A Review. *Fermentation* **2023**, *9*, 463. [[CrossRef](#)]

8. Martins, A.M.; Marto, J.M. A Sustainable Life Cycle for Cosmetics: From Design and Development to Post-Use Phase. *Sustain. Chem. Pharm.* **2023**, *35*, 101178. [[CrossRef](#)]
9. Cha, J.-Y.; Yang, H.-J.; Moon, H.-I.; Cho, Y.-S. Inhibitory Effect and Mechanism on Melanogenesis from Fermented Herbal Composition for Medical or Food Uses. *Food Res. Int.* **2012**, *45*, 225–231. [[CrossRef](#)]
10. Bijak, M. Silybin, a Major Bioactive Component of Milk Thistle (*Silybum marianum* L. Gaertn.)—Chemistry, Bioavailability, and Metabolism. *Molecules* **2017**, *22*, 1942. [[CrossRef](#)]
11. Mihailović, V.; Srećković, N.; Popović-Djordjević, J.B. Silybin and Silymarin: Phytochemistry, Bioactivity, and Pharmacology. In *Handbook of Dietary Flavonoids*; Xiao, J., Ed.; Springer: Cham, Switzerland, 2023; pp. 1–45, ISBN 978-3-030-94753-8.
12. Raclariu-Manolică, A.C.; Socaciu, C. Detecting and Profiling of Milk Thistle Metabolites in Food Supplements: A Safety-Oriented Approach by Advanced Analytics. *Metabolites* **2023**, *13*, 440. [[CrossRef](#)] [[PubMed](#)]
13. Chambers, C.S.; Holečková, V.; Petrásková, L.; Biedermann, D.; Valentová, K.; Buchtá, M.; Křen, V. The Silymarin Composition. . . and Why Does It Matter??? *Food Res. Int.* **2017**, *100*, 339–353. [[CrossRef](#)] [[PubMed](#)]
14. Schafer, N.; Balwierz, R.; Biernat, P.; Ochędzan-Siodłak, W.; Lipok, J. Natural Ingredients of Transdermal Drug Delivery Systems as Permeation Enhancers of Active Substances through the Stratum Corneum. *Mol. Pharm.* **2023**, *20*, 3278–3297. [[CrossRef](#)] [[PubMed](#)]
15. Sevinç-Özakar, R.; Seyret, E.; Özakar, E.; Adıgüzel, M.C. Nanoemulsion-Based Hydrogels and Organogels Containing Propolis and Dexpanthenol: Preparation, Characterization, and Comparative Evaluation of Stability, Antimicrobial, and Cytotoxic Properties. *Gels* **2022**, *8*, 578. [[CrossRef](#)] [[PubMed](#)]
16. Sannino, A.; Demitri, C.; Madaghiale, M. Biodegradable Cellulose-Based Hydrogels: Design and Applications. *Materials* **2009**, *2*, 353–373. [[CrossRef](#)]
17. Marceddu, R.; Dinolfo, L.; Carrubba, A.; Sarno, M.; Di Miceli, G. Milk Thistle (*Silybum marianum* L.) as a Novel Multipurpose Crop for Agriculture in Marginal Environments: A Review. *Agronomy* **2022**, *12*, 729. [[CrossRef](#)]
18. Gillessen, A.; Schmidt, H.H.-J. Silymarin as Supportive Treatment in Liver Diseases: A Narrative Review. *Adv. Ther.* **2020**, *37*, 1279–1301. [[CrossRef](#)] [[PubMed](#)]
19. Ghosh, A.; Ghosh, T.; Jain, S. Silymarin—A Review on the Pharmacodynamics and Bioavailability Enhancement Approaches. *J. Pharm. Sci. Technol.* **2010**, *2*, 348–355.
20. Javed, S.; Kohli, K.; Ahsan, W. Bioavailability Augmentation of Silymarin Using Natural Bioenhancers: An in Vivo Pharmacokinetic Study. *Braz. J. Pharm. Sci.* **2022**, *58*, e20160. [[CrossRef](#)]
21. Khazaei, R.; Seidavi, A.; Bouyeh, M. A Review on the Mechanisms of the Effect of Silymarin in Milk Thistle (*Silybum marianum*) on Some Laboratory Animals. *Vet. Med. Sci.* **2021**, *8*, 289–301. [[CrossRef](#)]
22. Kim, E.J.; Kim, J.; Lee, M.Y.; Sudhanva, M.S.; Devakumar, S.; Jeon, Y.J. Silymarin Inhibits Cytokine-Stimulated Pancreatic Beta Cells by Blocking the ERK1/2 Pathway. *Biomol. Ther.* **2014**, *22*, 282–287. [[CrossRef](#)] [[PubMed](#)]
23. Barnes, T.M.; Mijaljica, D.; Townley, J.P.; Spada, F.; Harrison, I.P. Vehicles for Drug Delivery and Cosmetic Moisturizers: Review and Comparison. *Pharmaceutics* **2021**, *13*, 2012. [[CrossRef](#)] [[PubMed](#)]
24. Bashir, S.; Fitaihi, R.; Abdelhakim, H.E. Advances in Formulation and Manufacturing Strategies for the Delivery of Therapeutic Proteins and Peptides in Orally Disintegrating Dosage Forms. *Eur. J. Pharm. Sci.* **2023**, *182*, 106374. [[CrossRef](#)] [[PubMed](#)]
25. Adepu, S.; Ramakrishna, S. Controlled Drug Delivery Systems: Current Status and Future Directions. *Molecules* **2021**, *26*, 5905. [[CrossRef](#)]
26. Burgess, J.L.; Wyant, W.A.; Abdo Abujamra, B.; Kirsner, R.S.; Jozic, I. Diabetic Wound-Healing Science. *Medicina* **2021**, *57*, 1072. [[CrossRef](#)]
27. Ashkani-Esfahani, S.; Emami, Y.; Esmailzadeh, E.; Bagheri, F.; Namazi, M.R.; Keshtkar, M.; Khoshneviszadeh, M.; Noorafshan, A. Silymarin Enhanced Fibroblast Proliferation and Tissue Regeneration in Full Thickness Skin Wounds in Rat Models: A Stereological Study. *J. Saudi Soc. Dermatol. Dermatol. Surg.* **2013**, *17*, 7–12. [[CrossRef](#)]
28. Makuch, E.; Ossowicz-Rupniewska, P.; Klebko, J.; Janus, E. Biodegradation of L-Valine Alkyl Ester Ibuprofenates by Bacterial Cultures. *Materials* **2021**, *14*, 3180. [[CrossRef](#)]
29. Bajpai, P. *Single Cell Protein Production from Lignocellulosic Biomass*; Springer: Berlin/Heidelberg, Germany, 2017; ISBN 978-981-10-5872-1.
30. Wijaya, H.; Sasaki, K.; Kahar, P.; Yopi, Y.; Kawaguchi, H.; Sazuka, T.; Ogino, C.; Prasetya, B.; Kondo, A. Repeated Ethanol Fermentation from Membrane-Concentrated Sweet Sorghum Juice Using the Flocculating Yeast *Saccharomyces Cerevisiae* F118 Strain. *Bioresour. Technol.* **2018**, *265*, 542–547. [[CrossRef](#)]
31. Lin, Y.; Yang, T.; Shen, L.; Zhang, J.; Liu, L. Study on the Properties of *Dendrobium officinale* Fermentation Broth as Functional Raw Material of Cosmetics. *J. Cosmet. Dermatol.* **2022**, *21*, 1216–1223. [[CrossRef](#)]
32. Makuch, E.; Nowak, A.; Günther, A.; Pelech, R.; Kucharski, Ł.; Duchnik, W.; Klimowicz, A. The Effect of Cream and Gel Vehicles on the Percutaneous Absorption and Skin Retention of a New Eugenol Derivative With Antioxidant Activity. *Front. Pharmacol.* **2021**, *12*, 658381. [[CrossRef](#)]
33. Nowak, A.; Zagórska-Dziok, M.; Ossowicz-Rupniewska, P.; Makuch, E.; Duchnik, W.; Kucharski, Ł.; Adamiak-Giera, U.; Prowans, P.; Czaplá, N.; Bargiel, P.; et al. *Epilobium angustifolium* L. Extracts as Valuable Ingredients in Cosmetic and Dermatological Products. *Molecules* **2021**, *26*, 3456. [[CrossRef](#)] [[PubMed](#)]

34. Makuch, E.; Nowak, A.; Günther, A.; Pelech, R.; Kucharski, Ł.; Duchnik, W.; Klimowicz, A. Enhancement of the Antioxidant and Skin Permeation Properties of Eugenol by the Esterification of Eugenol to New Derivatives. *AMB Expr.* **2020**, *10*, 187. [[CrossRef](#)] [[PubMed](#)]
35. Kucharski, Ł.; Cybulska, K.; Kucharska, E.; Nowak, A.; Pelech, R.; Klimowicz, A. Biologically Active Preparations from the Leaves of Wild Plant Species of the Genus *Rubus*. *Molecules* **2022**, *27*, 5486. [[CrossRef](#)] [[PubMed](#)]
36. Karamać, M.; Pegg, R.B. Limitations of the Tetramethylmurexide Assay for Investigating the Fe(II) Chelation Activity of Phenolic Compounds. *J. Agric. Food Chem.* **2009**, *57*, 6425–6431. [[CrossRef](#)] [[PubMed](#)]
37. Hossain, M.A.; Piyatida, P.; da Silva, J.A.T.; Fujita, M. Molecular Mechanism of Heavy Metal Toxicity and Tolerance in Plants: Central Role of Glutathione in Detoxification of Reactive Oxygen Species and Methylglyoxal and in Heavy Metal Chelation. *J. Bot.* **2012**, *2012*, e872875. [[CrossRef](#)]
38. Hellawell, J.M.; Abel, R. A Rapid Volumetric Method for the Analysis of the Food of Fishes. *J. Fish Biol.* **1971**, *3*, 29–37. [[CrossRef](#)]
39. Zhang, P.; Zhang, E.; Xiao, M.; Chen, C.; Xu, W. Enhanced Chemical and Biological Activities of a Newly Biosynthesized Eugenol Glycoconjugate, Eugenol α -D-Glucopyranoside. *Appl. Microbiol. Biotechnol.* **2013**, *97*, 1043–1050. [[CrossRef](#)]
40. Nowak, A.; Cybulska, K.; Makuch, E.; Kucharski, Ł.; Różewicka-Czabańska, M.; Prowans, P.; Czapla, N.; Bargiel, P.; Petriczko, J.; Klimowicz, A. In Vitro Human Skin Penetration, Antioxidant and Antimicrobial Activity of Ethanol-Water Extract of Fireweed (*Epilobium angustifolium* L.). *Molecules* **2021**, *26*, 329. [[CrossRef](#)]
41. Lorenzo, J.M.; Putnik, P.; Bursać Kovačević, D.; Petrović, M.; Munekata, P.E.; Gómez, B.; Marszałek, K.; Roohinejad, S.; Barba, F.J. Chapter 4—Silymarin Compounds: Chemistry, Innovative Extraction Techniques and Synthesis. In *Studies in Natural Products Chemistry; Bioactive Natural Products*; Atta-Ur-Rahman, A., Ed.; Elsevier: Amsterdam, The Netherlands, 2020; Volume 64, pp. 111–130.
42. Aiken, A.C.; DeCarlo, P.F.; Jimenez, J.L. Elemental Analysis of Organic Species with Electron Ionization High-Resolution Mass Spectrometry. *Anal. Chem.* **2007**, *79*, 8350–8358. [[CrossRef](#)]
43. Elmowafy, M.; Viitala, T.; Ibrahim, H.M.; Abu-Elyazid, S.K.; Samy, A.; Kassem, A.; Yliperttula, M. Silymarin Loaded Liposomes for Hepatic Targeting: In Vitro Evaluation and HepG2 Drug Uptake. *Eur. J. Pharm. Sci.* **2013**, *50*, 161–171. [[CrossRef](#)]
44. Goddard, J.M.; Hotchkiss, J.H. Polymer Surface Modification for the Attachment of Bioactive Compounds. *Prog. Polym. Sci.* **2007**, *32*, 698–725. [[CrossRef](#)]
45. de Castro, K.C.; Coco, J.C.; dos Santos, É.M.; Ataíde, J.A.; Martinez, R.M.; do Nascimento, M.H.M.; Prata, J.; da Fonte, P.R.M.L.; Severino, P.; Mazzola, P.G.; et al. Pluronic® Triblock Copolymer-Based Nanoformulations for Cancer Therapy: A 10-Year Overview. *J. Control Release* **2023**, *353*, 802–822. [[CrossRef](#)] [[PubMed](#)]
46. Gyles, D.A.; Castro, L.D.; Silva, J.O.C.; Ribeiro-Costa, R.M. A Review of the Designs and Prominent Biomedical Advances of Natural and Synthetic Hydrogel Formulations. *Eur. Polym. J.* **2017**, *88*, 373–392. [[CrossRef](#)]
47. Ziemlewska, A.; Nizioł-Łukaszewska, Z.; Zagórska-Dziok, M.; Bujak, T.; Wójciak, M.; Sowa, I. Evaluation of Cosmetic and Dermatological Properties of Kombucha-Fermented Berry Leaf Extracts Considered to Be By-Products. *Molecules* **2022**, *27*, 2345. [[CrossRef](#)]
48. Ogrodowczyk, A.M.; Kalicki, B.; Wróblewska, B. The Effect of Lactic Acid Fermentation with Different Bacterial Strains on the Chemical Composition, Immunoreactive Properties, and Sensory Quality of Sweet Buttermilk. *Food Chem.* **2021**, *353*, 129512. Available online: <https://pubmed.ncbi.nlm.nih.gov/33740512/> (accessed on 29 November 2023).
49. Mojović, L.; Pejin, D.; Grujić, O.; Markov, S.; Pejin, J.; Rakin, M.; Vukašinović, M.; Nikolić, S.; Savić, D. Progress in the Production of Bioethanol on Starch-Based Feedstocks. *Chem. Ind. Chem. Eng. Q. CICEQ* **2009**, *15*, 211–226. [[CrossRef](#)]
50. Ando, H.; Ryu, A.; Hashimoto, A.; Oka, M.; Ichihashi, M. Linoleic Acid and Alpha-Linolenic Acid Lightens Ultraviolet-Induced Hyperpigmentation of the Skin. *Arch. Dermatol. Res.* **1998**, *290*, 375–381. [[CrossRef](#)]
51. Chatatikun, M.; Tedsasen, A.; Pattarangoon, N.C.; Palachum, W.; Chuaijit, S.; Mudpan, A.; Pruksaphanrat, S.; Sohbenalee, S.; Yamasaki, K.; Klangbud, W.K. Antioxidant Activity, Anti-Tyrosinase Activity, Molecular Docking Studies, and Molecular Dynamic Simulation of Active Compounds Found in Nipa Palm Vinegar. *PeerJ* **2023**, *11*, e16494. Available online: <https://www.ncbi.nlm.nih.gov/pmc/articles/PMC10680452/> (accessed on 1 December 2023).
52. Lisov, N.; Čakar, U.; Milenković, D.; Čebela, M.; Vuković, G.; Despotović, S.; Petrović, A. The Influence of Cabernet Sauvignon Ripeness, Healthy State and Maceration Time on Wine and Fermented Pomace Phenolic Profile. *Fermentation* **2023**, *9*, 695. [[CrossRef](#)]
53. Bertges, F.S.; da Penha Henriques do Amaral, M.; Rodarte, M.P.; Vieira Fonseca, M.J.; Sousa, O.V.; Pinto Vilela, F.M.; Alves, M.S. Assessment of Chemical Changes and Skin Penetration of Green Arabica Coffee Beans Biotransformed by *Aspergillus oryzae*. *Biocatal. Agric. Biotechnol.* **2020**, *23*, 101512. [[CrossRef](#)]
54. Ossowicz-Rupniewska, P.; Bednarczyk, P.; Nowak, M.; Nowak, A.; Duchnik, W.; Kucharski, Ł.; Kleboko, J.; Świątek, E.; Bilska, K.; Rokicka, J.; et al. Evaluation of the Structural Modification of Ibuprofen on the Penetration Release of Ibuprofen from a Drug-in-Adhesive Matrix Type Transdermal Patch. *Int. J. Mol. Sci.* **2022**, *23*, 7752. [[CrossRef](#)]
55. Adamiak-Giera, U.; Nowak, A.; Duchnik, W.; Ossowicz-Rupniewska, P.; Czerkawska, A.; Machoy-Mokrzyńska, A.; Sulikowski, T.; Kucharski, Ł.; Białecka, M.; Klimowicz, A.; et al. Evaluation of the in Vitro Permeation Parameters of Topical Ketoprofen and Lidocaine Hydrochloride from Transdermal Pentravan® Products through Human Skin. *Front. Pharmacol.* **2023**, *14*, 1157977. [[CrossRef](#)]

56. Zillich, O.V.; Schweiggert-Weisz, U.; Hasenkopf, K.; Eisner, P.; Kerscher, M. Release and in vitro Skin Permeation of Polyphenols from Cosmetic Emulsions. *Int. J. Cosmet. Sci.* **2013**, *35*, 491–501. [[CrossRef](#)] [[PubMed](#)]
57. Nowak, A.; Zagórska-Dziok, M.; Perużyńska, M.; Cybulska, K.; Kucharska, E.; Ossowicz-Rupniewska, P.; Piotrowska, K.; Duchnik, W.; Kucharski, L.; Sulikowski, T.; et al. Assessment of the Anti-Inflammatory, Antibacterial and Anti-Aging Properties and Possible Use on the Skin of Hydrogels Containing *Epilobium Angustifolium* L. Extracts. *Front Pharmacol.* **2022**, *13*, 896706. [[CrossRef](#)] [[PubMed](#)]
58. Singh, R.P.; Agarwal, R. Cosmeceuticals and Silibinin. *Clin. Dermatol.* **2009**, *27*, 479–484. [[CrossRef](#)] [[PubMed](#)]
59. Rigon, C.; Marchiori, M.C.L.; da Silva Jardim, F.; Pegoraro, N.S.; dos Santos Chaves, P.; Velho, M.C.; Beck, R.C.R.; Ourique, A.F.; Sari, M.H.M.; de Oliveira, S.M.; et al. Hydrogel Containing Silibinin Nanocapsules Presents Effective Anti-Inflammatory Action in a Model of Irritant Contact Dermatitis in Mice. *Eur. J. Pharm. Sci.* **2019**, *137*, 104969. [[CrossRef](#)]
60. Micek, I.; Nawrot, J.; Seraszek-Jaros, A.; Jenerowicz, D.; Schroeder, G.; Spiżewski, T.; Suchan, A.; Pawlaczyk, M.; Gornowicz-Porowska, J. Taxifolin as a Promising Ingredient of Cosmetics for Adult Skin. *Antioxidants* **2021**, *10*, 1625. [[CrossRef](#)]
61. Rajnochová Svobodová, A.; Ryšavá, A.; Psotová, M.; Kosina, P.; Zálešák, B.; Ulrichová, J.; Vostálová, J. The Phototoxic Potential of the Flavonoids, Taxifolin and Quercetin. *Photochem. Photobiol.* **2017**, *93*, 1240–1247. [[CrossRef](#)]

Disclaimer/Publisher’s Note: The statements, opinions and data contained in all publications are solely those of the individual author(s) and contributor(s) and not of MDPI and/or the editor(s). MDPI and/or the editor(s) disclaim responsibility for any injury to people or property resulting from any ideas, methods, instructions or products referred to in the content.